SEISMIC TEST OF CONCRETE BLOCK INFILLED REINFORCED CONCRETE FRAMES

Yoshiaki NAKANO[1], Ho CHOI[2], Yasushi SANADA[3] and Naruhito YAMAUCHI[4]

[1] Associate Professor, Institute of Industrial Science, The University of Tokyo, Tokyo, Japan, iisnak@iis.u-tokyo.ac.jp
[2] Graduate Student, School of Engineering, The University of Tokyo, Tokyo, Japan, choiho@iis.u-tokyo.ac.jp
[3] Research Associate, Earthquake Research Institute, The University of Tokyo, Tokyo, Japan, ysanada@eri.u-tokyo.ac.jp
[4] Technical Associate, Institute of Industrial Science, The University of Tokyo, Tokyo, Japan, nyama@iis.u-tokyo.ac.jp

ABSTRACT: The objective of this study is to develop pre- and post-earthquake seismic evaluation method of concrete block infilled reinforced concrete frames. For this purpose, full-scale, one-bay, single-story specimens having different axial loads in columns and different opening configurations in wall are tested to investigate typical school buildings in Korea. In this paper, the relationship between observed damage and seismic performance is discussed primarily focusing on crack width in concrete block walls, load bearing capacity, and residual deformation.

Key Words: unreinforced concrete block (CB) wall, reinforced concrete frame, damage assessment, residual seismic capacity, crack width

INTRODUCTION

In some regions of Asia, Europe, and Latin America where earthquakes frequently occur, serious earthquake damage is commonly found resulting from catastrophic building collapse. Such damaged buildings often have unreinforced masonry (URM) walls, which are considered non-structural elements in the design stage, and building engineers therefore have paid less attention to their effects on structural performance although URM walls may interact with boundary frames as has been often found in the past damaging earthquakes.

After an earthquake, the major concerns to damaged buildings are their safety/risk to aftershocks, quantitative damage assessment to evaluate their residual seismic capacity and to identify necessary actions on the damaged buildings. Post-event damage evaluation is therefore essential for quick recovery of damaged community as well as pre-event seismic evaluation and strengthening of vulnerable buildings. Few investigations on masonry walls, however, have been made to quantitatively identify their damage level and criteria to judge necessary actions for their continued use, repair and rehabilitation.

In this study, reinforced concrete (RC) frames for school buildings in Korea, which typically have unreinforced concrete block (CB) walls, are experimentally investigated to develop pre- and post-earthquake seismic evaluation method. In the tests, full-scale, one-bay, single-story specimens having different axial loads in columns and different opening configurations in walls are tested under cyclic loading, and the contribution of unreinforced CB walls to overall behaviors, crack patterns in walls

and frames, and their crack widths which may be of great significance for post-event damage assessment are carefully observed.

In this paper, the relationship between observed damage and seismic performance is discussed primarily focusing on crack width in CB walls, load bearing capacity, and residual deformation.

OUTLINE OF EXPERIMENT

Test Specimen

Fig. 1 shows a standard design for Korean school buildings in the 1980s (The Ministry of Construction and Transportation (2002)). As can be found in this figure, unreinforced concrete block (CB) walls are commonly used as partition walls or exterior walls in Korean school buildings. In this study, 4 specimens reproducing a first or fourth story of 4 story RC school buildings are tested under cyclic loading. They are; infilled wall type 1 (designated as IW1) assuming a first story, infilled wall type 2 (IW2) assuming a fourth story, and wing wall type (WW) and partial height wall type (PW) both having opening in wall. The axial force applied in each column is 720 kN (4 N/mm^2) for specimens IW1, WW, and PW while 180 kN (1 N/mm^2) for IW2.

The design details of specimen IW1 are shown in Fig. 2. Since seismic design provisions for buildings were introduced in 1988 in Korea, the model structures studied herein are not designed to seismic loads. Therefore, they have (1) large spacing of hoops (300 mm) and (2) 90 degree hook at both ends of hoops as shown in the figure. Specimens IW1, WW, and PW have identical re-bar arrangement in columns but different wall arrangement, while IW2 has fewer re-bars than other 3 specimens. Concrete block units are laid in the RC frame after concrete is hardened. All specimens are fabricated and tested at RIST (Research Institute of Industrial Science and Technology) in Korea to follow the Korean construction practice.

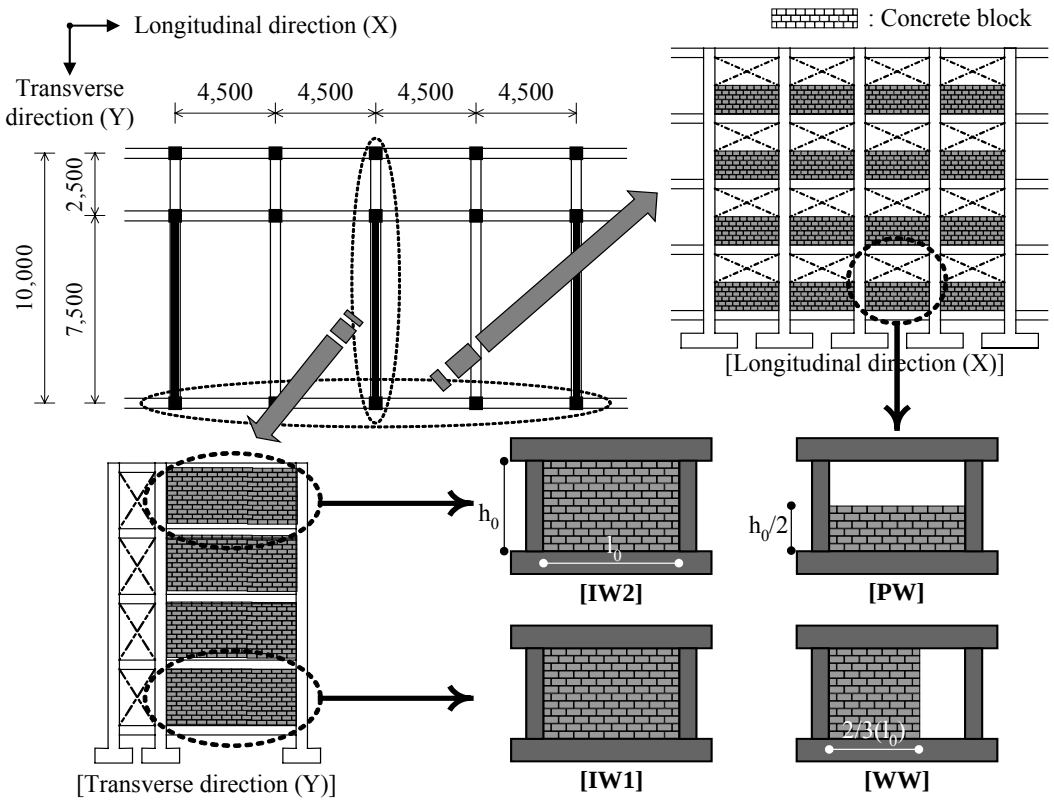

Fig. 1 Standard design of Korean school buildings in the 1980s and specimen plan

Material Characteristic

Material test results are shown in Tables 1 through 3 (the average value of three samples is shown in Tables). Although the design strength of concrete specified in the standard design of Korean school buildings in the 1980s is 21 N/mm^2, the compressive strength of test pieces exceeds the design value as shown in Table 1. The deformed bar SD40 (nominal yield strength: 395 N/mm^2) is used for longitudinal and shear reinforcement. The size of a CB unit is 390×190×190 mm. It has three hollows inside and a half-sized hollow on both ends as shown in Fig. 2. Joint mortar having the cement-to-sand ratio of 1:3.5, which is generally used in Korea, is placed horizontally and vertically between CB units in wall.

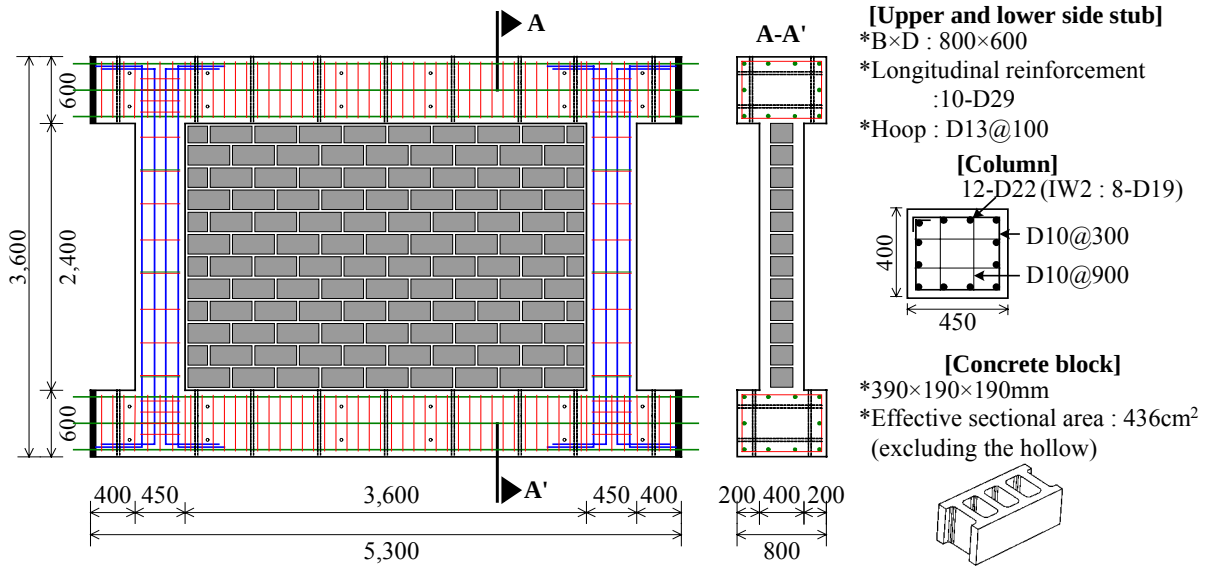

Fig. 2 Detail of specimen (IW1)

Table 1 Mechanical properties of concrete

Specimen	Compressive strength (N/mm^2)	Young's modulus (N/mm^2)	Split tensile strength (N/mm^2)	Specimen	Compressive strength (N/mm^2)	Young's modulus (N/mm^2)	Split tensile strength (N/mm^2)
IW1	27.3	2.28×10^4	2.4	WW	23.8	2.11×10^4	2.0
IW2	29.6	2.30×10^4	2.4	PW	26.1	2.03×10^4	2.2

Table 2 Mechanical properties of reinforcement

Bar	Use / Member	Yield strength (N/mm^2)	Tensile strength (N/mm^2)	Young's modulus (N/mm^2)
D10	Hoop / Column	404	581	1.91×10^5
D13	Stirrup / Stub	419	622	1.88×10^5
D19	Longitudinal reinforcement of IW2 / Column	432	599	1.95×10^5
D22	Longitudinal reinforcement of IW1, WW, PW / Column	498	598	1.88×10^5
D29	Longitudinal reinforcement / Stub	455	-*	2.09×10^5

* strain not measured due to displaced gauge

Table 3 Mechanical properties of concrete block and joint mortar

Concrete block				Joint mortar	
Block unit*		Block prism**			
Compressive strength (N/mm^2)	Young's modulus (N/mm^2)	Compressive strength (N/mm^2)	Young's modulus (N/mm^2)	Compressive strength (N/mm^2)	Young's modulus (N/mm^2)
27.0	2.14×10^4	17.5	1.22×10^4	22.1	1.47×10^4

* Excluding hollow area ** 3 layered specimen

Test Setup and Test Program

Fig. 3 and Photo 1 show the loading system. Push and pull lateral loads are applied to each specimen through a loading beam tightly fastened to the specimen. Fig. 4 shows the loading history, where a peak drift angle *R* is defined as "lateral displacement/column height". As shown in the figure, peak drift angles of 1, 2, 4, 6.7, 10, and 20×10^{-3} rad. are planned and 2.5 cycles for each peak drift are imposed to eliminate one-sided progressive failure (unsymmetric failure pattern either in positive or negative loadings). It should be also noted that a 4×10^{-3}rad. loading is imposed after 10×10^{-3}rad. to investigate the effect of small amplitude loading after large deformation (i.e., aftershocks). After severe damage is found, the specimen is pushed over till collapse. A constant axial load of 1,440 kN (720 kN for each column) is applied to specimens IW1, WW, and PW while 360 kN (180 kN for each) to specimen IW2.

The measurement system is shown in Fig. 5. The relative lateral displacement between upper and lower stub, the vertical displacement of each column, and the diagonal deformation of frame and CB wall are measured. To measure the curvature distribution in column, displacement transducers are attached on both sides of each column at an interval of 150 mm (600 mm in the mid-column). Strains on major portions of longitudinal and shear reinforcement in columns are measured. In order to calculate the axial force carried by the CB wall, strain gauges are attached on both surfaces of 3 units in the uppermost layer immediately below the top stub. The relation between axial stress and strain is pre-determined from material testing of CB unit. From this result and strains measured during the experiment, the axial stress in CB wall is calculated. Maximum crack widths at peak loads and residual crack widths at unloaded stages are carefully measured in RC columns and CB wall.

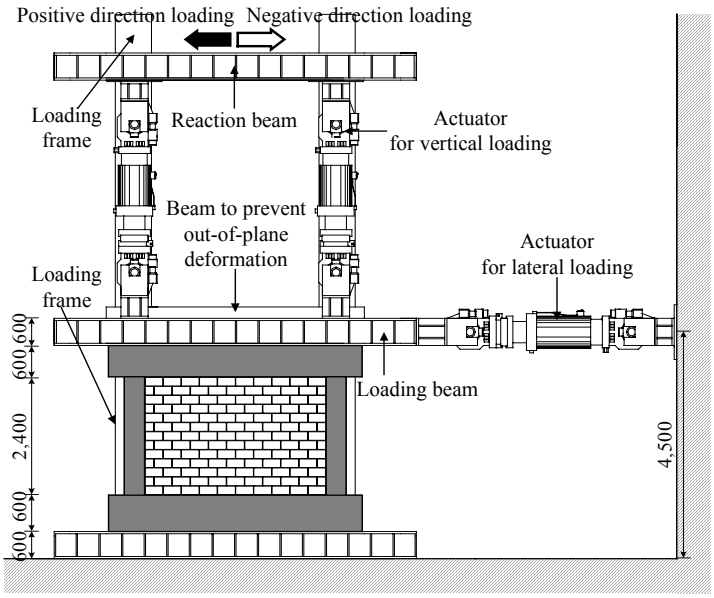

Fig. 3 Test setup

Photo 1 General view of test setup

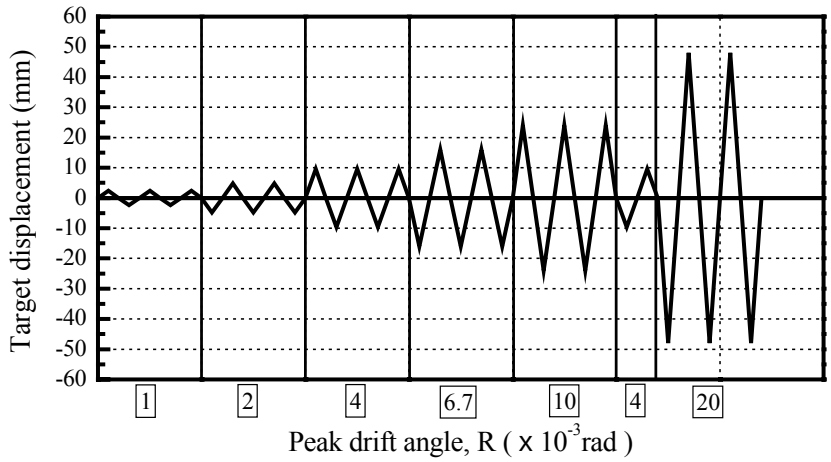

Fig. 4 Loading history

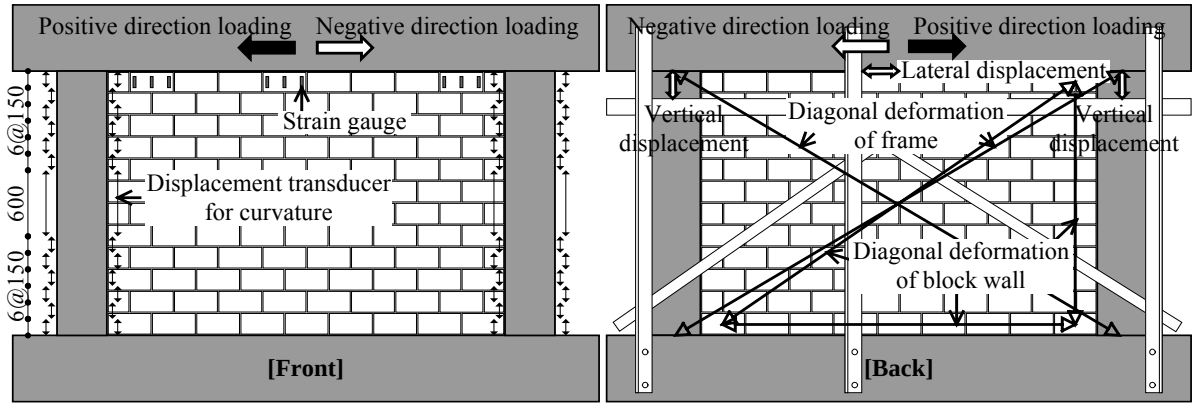

Fig. 5 Measurement system

TEST RESULTS

Failure Patterns

Fig. 6 shows the crack pattern of each specimen at the first cycle with peak drift angle of $+10\times10^{-3}$rad., which may facilitate to understand the resistance mechanism in the specimens. It should be noted that the specimens finally fail during the subsequent loading stage with larger amplitude. The failure pattern observed in each specimen is briefly described below.

Specimen IW1

Specimen IW1 has flexural cracks in RC column, and vertical and horizontal cracks in joint mortar between CB units at the first cycle of $+1\times10^{-3}$rad. During 2×10^{-3}rad. loading, the cracks develop and some cracks in joint mortar extend diagonally in CB units. At the first cycle of $+4\times10^{-3}$rad., clear shear cracks in both columns and wider cracks in CB wall are observed although few cracks are newly found in the wall. During 6.7×10^{-3}rad. loading, the flexural and shear cracks previously observed in columns significantly develop and stair-stepped diagonal cracks running through the wall center are observed. Since the shear cracks in the column base of compression side rapidly open at -15×10^{-3}rad., the test is terminated after 1.5 cycles of 15×10^{-3}rad. loading.

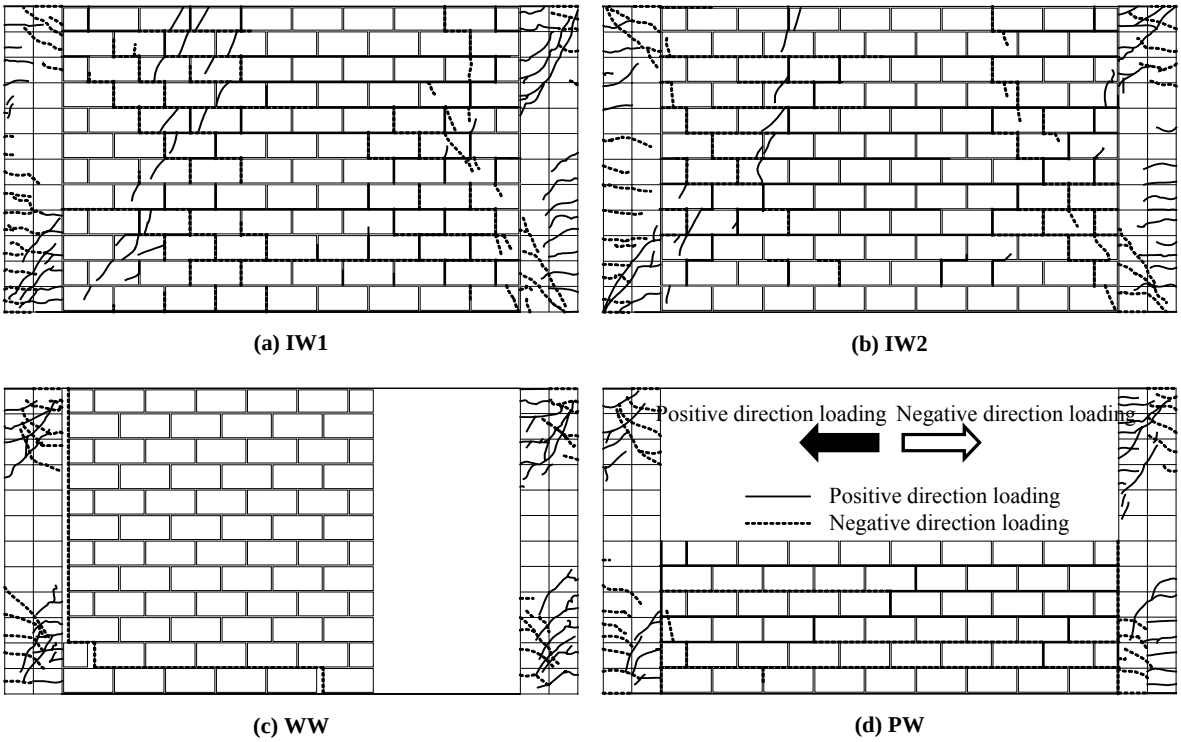

Fig. 6 Cracks in RC columns and CB wall at the 1st cycle with peak drift angle of $+10\times10^{-3}$rad.

Specimen IW2

Specimen IW2 has a crack pattern in both columns and wall, which is almost the same as that of specimen IW1. Although the strength deterioration is observed at the first cycle of $+20\times10^{-3}$rad., a rapid increase in crack width is not found. Since the shear crack in the column base of compression side rapidly open at $+33.3\times10^{-3}$rad., the experiment is terminated.

Specimen WW

Specimen WW has flexural cracks in column at the first cycle of $+1\times10^{-3}$rad. as is also found in specimen IW1. Since the specimen has a door opening and the CB wall end of the opening side is not directly confined by the column, stair-stepped diagonal cracks do not develop during the positive direction loading, and the whole CB wall gradually slides to the right (opening side) during cyclic loading causing separation of CB units and the left side column. Since the CB wall acts as a compressive strut in specimens IW1 and IW2, both of which have no opening, stair-stepped cracks diagonally run in the wall extending through the bottom of compression column and the top of tensile column as shown in Fig. 6(a) and (b). The wall of specimen WW is, however, much less confined by the boundary frame and does not contribute to the frame's lateral resistance. The specimen therefore behaves much like a bare frame and the shear cracks occur on both ends of columns simultaneously. At the first cycle of -20×10^{-3}rad., a shear crack in the column grows to 8 mm wide and the strength deteriorates during the following loading although it does not increase in width.

Specimen PW

Specimen PW has 2 major cracks horizontally crossing the mid-wall at 2.0×10^{-3}rad., and then the wall is divided into 3 layers of CB units. Shear cracks in the column base of compression side are observed at the first cycle of $+4\times10^{-3}$rad. During 6.7×10^{-3}rad. loading, cracks are observed in the entire bed joint

(horizontal joint) of the CB wall causing slippage at the joint interface. Since the shear failure is observed simultaneously at -16×10^{-3}rad. both in the column base of compression side and the column top of tension side, the experiment is terminated.

The Relation of Lateral Strength and Drift Angle

Fig. 7 shows the relation between the lateral strength and the drift angle of each specimen. The relation of maximum strength of overall frame, load-deflection curve, and the average shear stress of CB wall in each specimen is briefly described below.

Specimen IW1

The maximum strength of 960 kN is recorded at the first cycle of $+6.7\times10^{-3}$rad. and no remarkable strength deterioration is found until 13.3×10^{-3}rad. The shear cracks at the column base of compression side rapidly open at -15×10^{-3}rad., and the lateral load carrying capacity deteriorates to about 80% of the peak value as shown in Fig. 7. The load-deflection curve and crack patterns indicate that the specimen finally fails in shear due to shear force acting on the column base of the compression side after yield hinges are formed at both ends of the columns.

To investigate the contribution of CB wall to the lateral resistance of the specimen, the strength of bare frame is calculated and compared with test results as plotted in Fig. 7, where a plastic hinge zone is assumed over a distance of *D* (*D*: column depth, 450 mm) at both ends in columns. The strength of

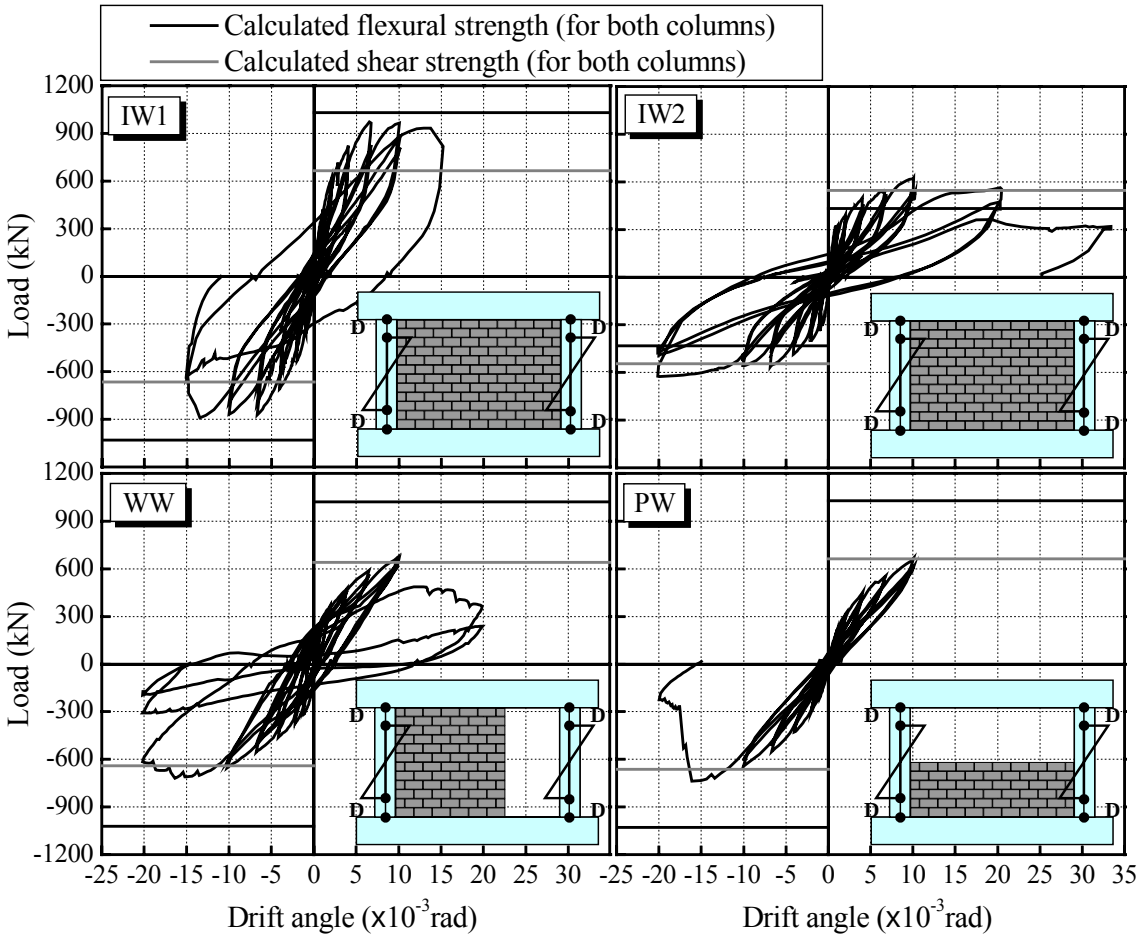

Fig. 7 Load vs. drift angle of each specimen

overall frame obtained from the experiment is about 1.4 times of the calculated shear strength (AIJ (1988)), which agrees well with the test results of specimens WW and PW as discussed subsequently, and the CB wall greatly contributes to the frame strength unless the wall causes out-of-plane failure. Assuming the discrepancy between the observed peak load and the calculated shear strength is carried by the CB wall, the average shear stress τ to the sectional area A including hollow (A=390× 190 mm) is approximately 0.4 N/mm^2.

Specimen IW2

The maximum strength of 630 kN is recorded at the first cycle of $+10\times10^{-3}$rad. Although the strength decreases slightly at the first cycle of $+20\times10^{-3}$rad., no remarkable strength deterioration is found until 33.3×10^{-3}rad., and the stable lateral load carrying capacity is maintained until final loading. Since the specimen has the lower axial force level and fewer longitudinal re-bars, it has lower strength but higher ductility than specimen IW1. The strength of overall frame obtained from the experiment is about 1.5 times of the calculated flexural strength and the average shear stress τ of the CB wall is approximately 0.3 N/mm^2.

Specimen WW

The maximum strength of 734 kN is recorded at -16×10^{-3}rad., which is far less than that of specimen IW1 having no opening but the same axial force level. As mentioned earlier, since the specimen has a door opening, the CB wall is much less confined by the boundary frame and does not contribute to the frame's lateral resistance. Therefore, the strength of overall frame obtained from the experiment is about 1.1 times of the calculated shear strength, which demonstrates that the specimen's behavior is similar to a bare frame and it is highly dependent on the opening configuration in wall.

Specimen PW

The maximum strength of 744 kN is recorded at -16×10^{-3}rad. and the shear failure simultaneously occurs in the column base of compression side and the column top of tension side. Since the entire bed joint is through-cracked, each CB unit slides at the cracked interface. The columns are, therefore, less interacted with the CB wall and the specimen demonstrates a behavior similar to a bare frame. The strength of overall frame obtained from the test corresponds well with the calculated shear strength.

CRACK WIDTHS AND RESPONSE OF SPECIMENS

Measurement of Crack Width

Cracks in members after an earthquake are visible and essential evidence of damage that can be found at the building site, and they often provide valuable information regarding the response that the building has experienced and its residual capacity. To investigate the relationship between damage and structural response, crack widths in RC columns and CB walls are carefully measured at peak loads and unloaded stages. Fig. 8 shows the measurement points in columns and walls made in this study.

The widths of flexural and shear cracks observed at the top and bottom of each column are measured. Since the crack widths are not necessarily uniform along the crack, its major width which is deemed to be largest along a crack is measured in its perpendicular direction. During and after 10×10^{-3}rad. loading, major 6 large cracks (3 cracks for flexure and 3 cracks for shear) are measured at both ends of each column to save crack observation time.

The widths of stair-stepped diagonal cracks running through the wall are also measured. During and after 10×10^{-3}rad. loading, major wide cracks found in the head joints of one continued crack are selectively measured to record the lateral dislocation of CB units (see Fig. 8(a)) while several cracks in the bed joints of one continued crack are measured to investigate a rotational behavior of wall (see Fig.

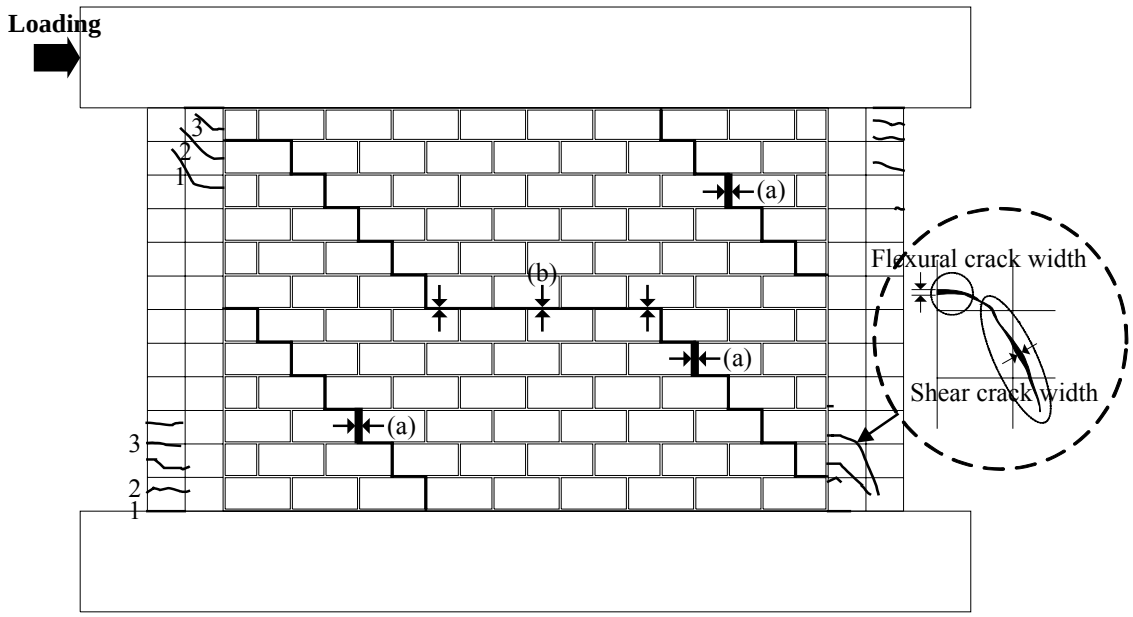

Fig. 8 Schematic illustration of measured points

8(b)). In the following sections, crack widths measured in the head joints are investigated for CB walls.

Crack Width of Concrete Block Wall at Peak Load

The measured results on lateral displacement (δ_p), total crack width (ΣW_p) and maximum crack width ($_{max}W_p$) of CB wall at positive peak loads for specimens IW1, IW2, and WW are plotted with respect to the peak drift angle in Fig. 9. Since the similar results are obtained in the subsequent cycles, only the results in the first cycle are plotted. For specimens IW1 and IW2, the relationship between the total crack widths (ΣW_p) and the maximum crack width ($_{max}W_p$) at peak loads is similar (i.e., $\Sigma W_p \approx {}_{max}W_p$) until 10×10^{-3}rad. because one major stair-stepped diagonal crack running through the wall represents the crack pattern of overall CB wall as previously mentioned. For specimen WW, one major L-shaped crack separates the CB wall from the adjacent RC column, as shown in Fig. 6(c), and the crack between them represents the damage to the wall (i.e., $\Sigma W_p \approx {}_{max}W_p$). The cracks developed during the

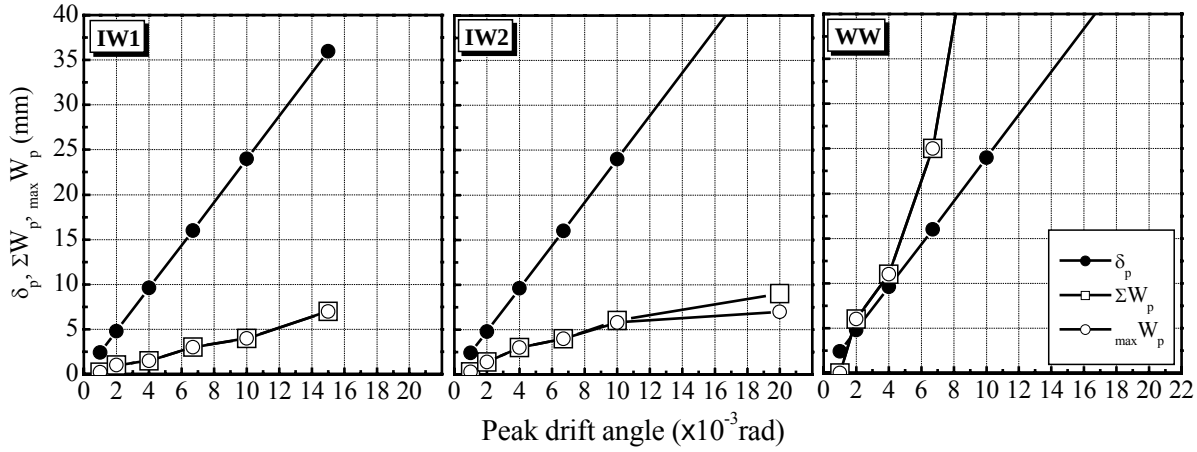

Fig. 9 δ_p, ΣW_p, and $_{max}W_p$ vs. peak drift angle (CB wall)

positive loading, however, do not close and their accumulated width tends to be wider than the peak displacement δ_p as shown in Fig. 9.

A crack width distribution in CB wall of specimens IW1 and IW2 is then estimated from flexural deformation distribution δ_f, shear deformation distribution δ_s, and overall lateral displacement δ_p in the following procedure. Fig. 10 illustrates the outline of the estimation procedure.

(1) Flexural deformation distribution

The distributions of flexural deformation in two RC columns along their height, ${}_t\delta_f(x)$ and ${}_c\delta_f(x)$, are computed based on the measured curvature distribution, where "t" and "c" denote "tension" side and "compression" side, and "x" denotes the distance from the top of each column, respectively.

(2) Shear deformation distribution

Assuming that the discrepancy between $\delta_f(0)$ and δ_p is shear deformation caused in the column, and that the shear deformation is linearly distributed over the top 1.5*D* for tension side column and the bottom 1.5*D* for compression side column, the shear deformation distribution can be obtained as shown below.

$$
\begin{aligned}
{}_t\delta_s(x) &= (\delta_p - {}_t\delta_f(0)) \cdot \frac{1.5D - x} {1.5D} && (0 \le x < 1.5D) \\
&= 0 && (1.5D \le x)
\end{aligned}
$$

$$
\begin{aligned}
{}_c\delta_s(x) &= (\delta_p - {}_c\delta_f(0)) && (0 \le x < h_0 - 1.5D) \\
&= (\delta_p - {}_c\delta_f(0)) \cdot \frac{h_0 - x} {1.5D} && (h_0 - 1.5D \le x \le h_0)
\end{aligned}
$$

where,

δ_p	: lateral displacement at the top of the specimen
${}_t\delta_f(x)$, ${}_c\delta_f(x)$	: flexural deformation distribution along column height
${}_t\delta_s(x)$, ${}_c\delta_s(x)$	: shear deformation distribution along column height
h_0	: column clear height (=2,400 mm)
x	: distance from column top
D	: column depth (=450 mm)

(3) Column deformation distribution

The deformation distribution $\delta(x)$ along each column then can be written as defined below.

$$
\begin{aligned}
{}_t\delta(x) &= {}_t\delta_f(x) + {}_t\delta_s(x) \\
{}_c\delta(x) &= {}_c\delta_f(x) + {}_c\delta_s(x)
\end{aligned}
$$

(4) Crack width distribution

Assuming that the discrepancy of deformation in two columns corresponds to the crack width in CB wall, the crack width distribution $W_p(x)$ and its maximum value ${}_{max}W_p(x)$ can be expressed as:

$$
\begin{aligned}
W_p(x) &= {}_c\delta(x) - {}_t\delta(x) \\
{}_{max}W_p &= max\ of\ [W_p(x)]
\end{aligned}
$$

Fig. 11 shows the relationship of maximum crack width ${}_{max}W_p$ between the measured and the computed values at peak loads of 1×10^{-3}rad. to 10×10^{-3}rad. loading. It should be noted that the relation of the *measured* total crack width ΣW_p and the *computed* ${}_{max}W_p$ is similar to that shown in Fig. 11 because the *measured* ΣW_p closely approximates *measured* ${}_{max}W_p$ as shown in Fig. 9. As can be found

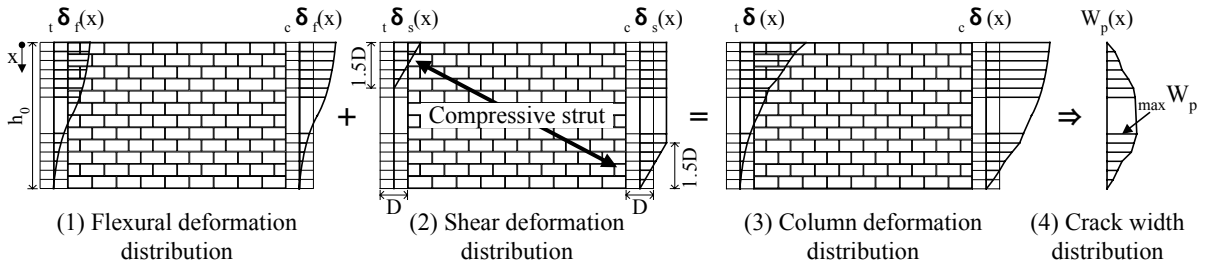

Fig. 10 Deformation distribution assumed in frame

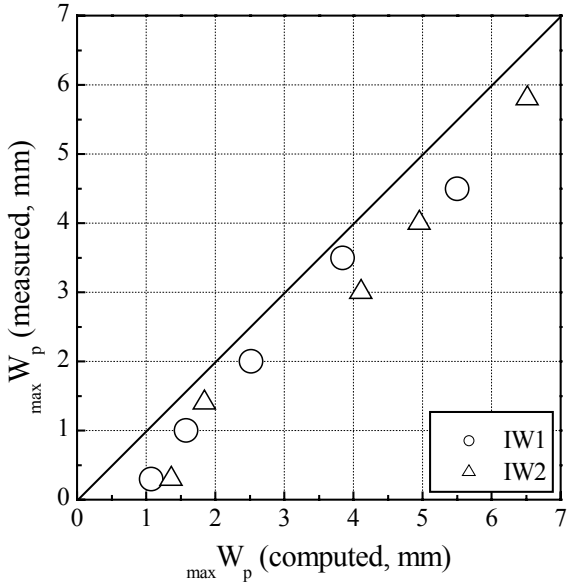

Fig. 11 Comparison of computed and measured maximum crack width of CB wall

in Fig. 11, the proposed method can roughly estimate the crack width in CB wall, although it slightly tends to overestimate the observed results.

Residual Crack Width at Unloaded Stage

The measured results on residual displacement (δ_0), total residual crack width (ΣW_0) and maximum residual crack width ($_{max}W_0$) of CB wall at unloaded stages in the positive loading for specimens IW1, IW2, and WW are plotted in Fig. 12. For specimens IW1 and IW2, the relationship between the total residual crack widths (ΣW_0) and the maximum residual crack width ($_{max}W_0$) is similar (i.e., $\Sigma W_0 \approx {}_{max}W_0$) until 10×10^{-3}rad. because one major stair-stepped diagonal crack running through the wall represents the crack pattern of overall CB wall. For specimen WW, one major L-shaped crack separates the CB wall from the adjacent RC column and the crack between them represents the damage to the wall (i.e., $\Sigma W_0 \approx {}_{max}W_0$). The cracks developed during the positive loading, however, do not close and their accumulated width tends to be wider than the residual displacement δ_0 as shown in Fig. 12. These tendencies are, as stated earlier, similar to those found in the relation at peak loads.

Fig. 13(a) and (b) show the ratio of maximum residual crack width to maximum crack width at peak loads ($_{max}W_0$ / $_{max}W_p$) and the ratio of maximum residual crack width to lateral displacement at peak loads ($_{max}W_0$ / δ_p), respectively. As shown in Fig. 13(a), the ratios of [$_{max}W_0$ / $_{max}W_p$] of specimens IW1 and IW2 are about 0.2 until 10×10^{-3}rad. before column failure because the columns confine the

CB wall and they help cracks in wall close during unloading. On the other hand, the ratios of specimen WW are much higher than those of IW1 and IW2 and they approach 1.0 because the cracks tend to be left open due to less confinement by the boundary frame. The ratios of [$_{max}W_0$ / δ_p] are accordingly close to 1.0 in specimen WW as shown Fig. 13(b) until 6.7×10^{-3}rad. loading, while they are much smaller in specimens IW1 and IW2.

After an earthquake, the major concern to damaged buildings is to evaluate their residual seismic capacity for continued use, repair and rehabilitation. Since the residual displacement δ_0 is likely to be related to the residual seismic capacity, the relation between δ_0 and the residual crack width, which may be closely correlated with δ_0 and can be directly measured at a damaged building site, is then investigated. Fig. 14 shows the ratio of maximum residual crack width to residual displacement ($_{max}W_0$ / δ_0) for specimens IW1 and IW2, where cracks in head joints in CB wall and flexural cracks in the left column are used in computing $_{max}W_0$. As can be found in the figure, the ratios in CB wall show relatively more stable values than those in the RC column, and therefore can be used to estimate the residual displacement δ_0 of the specimen with CB wall.

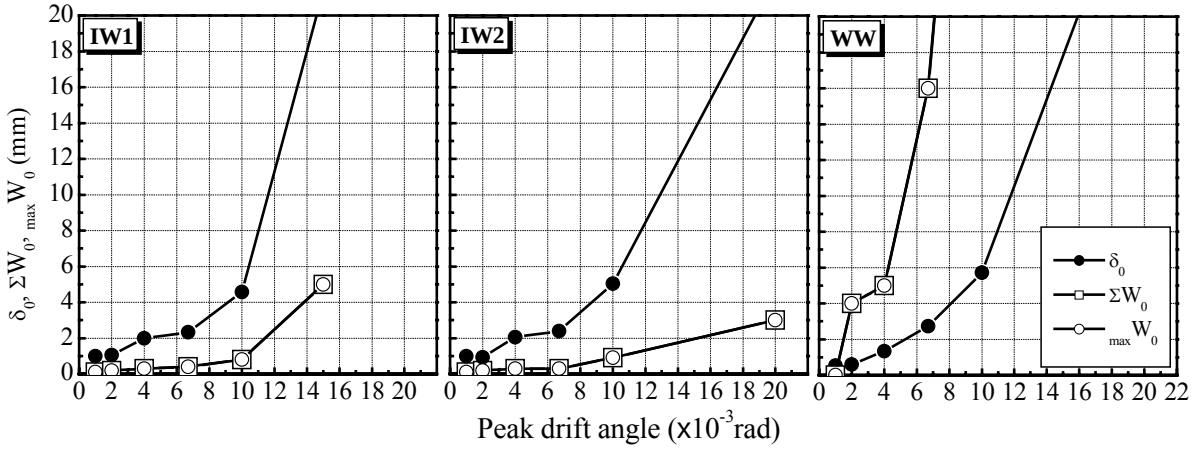

Fig. 12 δ_0, ΣW_0, and $_{max}W_0$ vs. peak drift angle (CB wall)

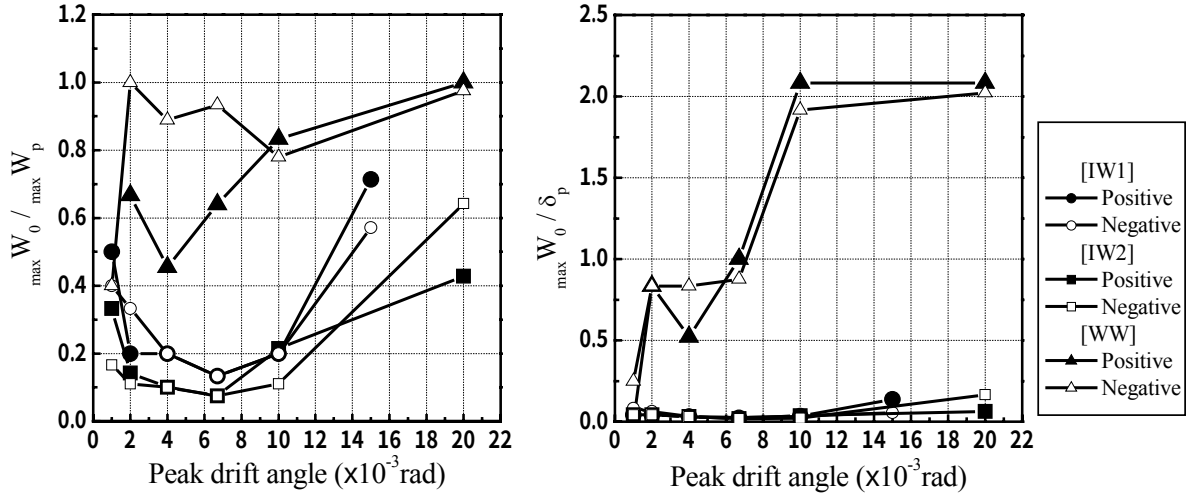

(a) $_{max}W_0$ / $_{max}W_p$ (b) $_{max}W_0$ / δ_p

Fig. 13 [$_{max}W_0$ / $_{max}W_p$] and [$_{max}W_0$ / δ_p] vs. peak drift angle (CB wall)

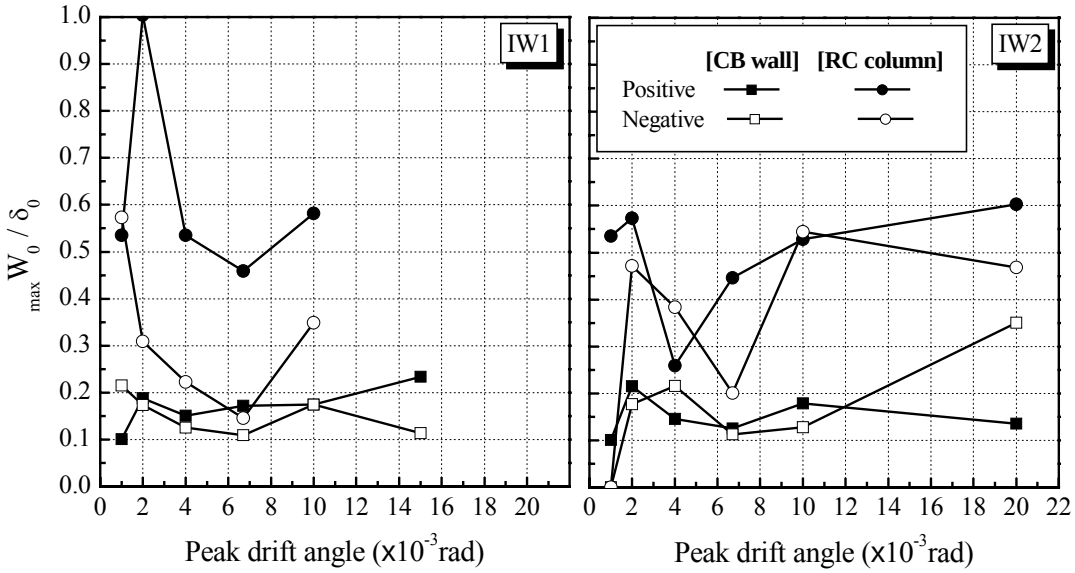

Fig. 14 $[_{max}W_0 / \delta_0]$ vs. peak drift angle

CONCLUSIONS

Seismic performance of unreinforced concrete block (CB) infilled RC frames for school buildings in Korea are experimentally investigated under cyclic loading, and the contribution of CB walls to overall behaviors, crack patterns and widths in walls and frames, and the correlation between their width and frame's displacement are discussed. The major findings can be summarized as follows.

(1) Specimens IW1 and IW2 having no opening finally fails in shear due to shear force acting on the column base of the compression side after yield hinges are formed at both ends of the columns. Specimen WW having a door opening behaves much like a bare frame and the shear cracks occur on both ends of columns simultaneously since the CB wall is much less confined by the boundary frame and does not contribute to the frame's lateral resistance. Specimen PW having a window opening also demonstrates a behavior similar to a bare frame since the columns are less interacted with the wall due to slippage at horizontal interface between each CB unit.

(2) The strength of overall frame in specimens IW1 and IW2 is about 1.4 and 1.5 times of the calculated strength of a bare frame, respectively, and the CB wall greatly contributes to the frame strength, while the strength in specimens WW and PW corresponds well with the calculated shear strength of a bare frame due to opening in the wall. The average shear stress τ of CB wall is 0.4 and 0.3 N/mm^2 in specimens IW1 and IW2, respectively.

(3) The crack width distribution in CB wall of specimens IW1 and IW2 is estimated from flexural deformation distribution δ_f, shear deformation distribution δ_s, and overall lateral displacement δ_p. The proposed method can roughly estimate the crack width in CB wall, although it slightly tends to overestimate the observed results.

(4) At peak loads until 10×10^{-3}rad. loading, specimens IW1, IW2, and WW have the maximum crack width $_{max}W_p$ similar to the total crack width ΣW_p. This is because one major stair-stepped diagonal crack running through the wall represents the crack pattern of overall CB wall in specimens IW1 and IW2, and one major L-shaped crack separates the CB wall from the adjacent RC column and the crack between them represents the damage to the CB wall in specimen WW. The similar tendencies are also found in the relation of residual crack width ΣW_0 and $_{max}W_0$.

(5) The ratios of maximum residual crack width to maximum crack width at peak loads ($_{max}W_0$ / $_{max}W_p$) in CB wall of specimens IW1 and IW2 are about 0.2 until 10×10^{-3}rad. before column failure because the columns confine the wall and they help cracks in wall close during unloading, while the ratios of specimen WW approach 1.0 because the cracks tend to be left open due to less confinement by the boundary frame. The ratios of maximum residual crack width to lateral displacement at peak loads ($_{max}W_0$ / δ_p) are accordingly close to 1.0 in specimen WW, while they are much smaller in specimens IW1 and IW2.

(6) The ratios of maximum residual crack width in CB wall to residual displacement ($_{max}W_0$ / δ_0) for specimens IW1 and IW2 show relatively more stable values than those in the RC column, and therefore can be used to estimate the residual displacement δ_0 of the specimen with CB wall.

ACKNOWLEDGMENT

The research reported herein was performed in cooperation with Professor Waon-Ho Yi of the Kwangwoon University and Dr. Sang-Hoon Oh of RIST (Research Institute of Industrial Science and Technology) in Korea. Technical supports organized by Mr. Young-Ki Kim, the Quality Manager at RIST, greatly contributed to solving various problems that were encountered during experiment. The authors express their deepest gratitude to all these supports without which the test was not accomplished.

REFERENCES

The Ministry of Construction and Transportation (2002). “A study on the seismic evaluation and retrofit of low-rise RC buildings in Korea.” 113-155.

Architectural Institute of Japan (1988). “Standard for structural calculation of reinforced concrete structures -Based on allowable stress concept-.” 167-192.